Applied Catalysis B: Environmental 221 (2018) 258–265

Contents lists available at ScienceDirect

Applied Catalysis B: Environmental

journal homepage: www.elsevier.com/locate/apcatb

Research paper

Wavelength dependence of the efficiency of photocatalytic processes for water treatment

Miguel Martín-Sómer, Beatriz Vega, Cristina Pablos, Rafael van Grieken, Javier Marugán*

Department of Chemical and Environmental Technology, ESCET, Spain
Universidad Rey Juan Carlos, C/ Tulipán s/n, 28933, Móstoles, Madrid, Spain

ARTICLE INFO

Keywords:
Iron citrate
TiO_2
Action spectra
LED
Sunlight

ABSTRACT

The main objective of this work is to present a novel approach to evaluate quantitatively the action spectra and energy efficiency for chemical oxidation and bacterial inactivation of photocatalytic processes using monochromatic LED sources. Two different catalysts with different absorption spectra (TiO_2 and iron citrate complex) were used. In all cases, it was confirmed a direct relationship between the absorption spectrum of the catalyst and the spectral dependence of the photonic efficiency. The best alternative for TiO_2 processes in terms of energy consumption when using artificial lighting is the use of 365 nm. In contrast, for iron complexes it seems more economically feasible the use of longer wavelengths close to the visible range, because the lower absorption of the complex is counterbalanced by the higher energy efficiency of the LED devices. This can be obviously extrapolated to the use of sunlight, where the use of iron-based photocatalytic processes can harvest a higher fraction of the available light. Predictions of the process efficiency under solar irradiation based on the action spectra determined with LED at laboratory scale have been successfully validated by experimental data. The methodology proposed in this work could be easily extrapolated to other wavelength ranges required by novel catalysts or efficient short wavelength monochromatic LED sources available in the future.

1. Introduction

TiO_2 has been widely used as photocatalyst due to its low cost and non-toxicity [1,2]. However one of the main drawbacks of TiO_2 photocatalysis is its relatively high band gap energy (above 3.0 eV for rutile and 3.2 eV for anatase) which requires wavelength below 400 nm, in the UV-A range [3]. Although the effectiveness of the use of sunlight as radiation source for the removal of pollutants has been extensively proved [4,5], since the solar spectrum reaching the Earth's surface contains only 5–7% in the UV region, solar photocatalysis with TiO_2 is limited to areas of the planet with very long periods of sun exposure and high radiation levels. Some authors have pointed out the possibility of doping TiO_2 with other compounds to expand their absorption spectrum [6]. Although its effectiveness in the visible range has been demonstrated [7–9], the synthesis of this type of catalysts would considerably increase the complexity and the costs of the process.

Another possibility for photocatalytic processes is the use of artificial light. The use of this type of illumination has been widely studied; however, it has not been implanted at industrial level because it is strongly limited by the energy consumption. In recent years, the development of LED technology has opened the possibility of implementing the process at industrial level due to the large energy savings compared to traditional lighting systems [10–14].

Additionally, the development of LED technology has derived in the availability of monochromatic light sources with different wavelengths [10]. The possibility of using wavelengths closer to the visible range has the advantage of showing significantly higher energy efficiency [15]. Therefore, the possibility of using catalysts active in the UV-A/Vis range such iron-based complexes in photo-Fenton processes is interesting not only from the possible use of solar light but also for the improvement in the energy efficiency of LED driven processes. However the photo-Fenton processes have the drawback of working at low pH levels in order to avoid the catalyst precipitation which limits its applications, especially for disinfection purposes [16–18]. An interesting alternative to consider is the use of iron–based complexes that do not precipitate at neutral pH such as the iron citrate complex (Fe-citrate). The effectiveness of Fe-citrate has recently been successfully tested for the treatment of both synthetic [19,20] and real water [16,21].

This work reports a novel approach for the quantitative evaluation of the action spectra and energy efficiency of TiO_2 and iron-based photocatalytic processes based on the use of monochromatic LED sources. Comparable LED based systems providing maximum emission

* Corresponding author.
E-mail address: javier.marugan@urjc.es (J. Marugán).

http://dx.doi.org/10.1016/j.apcatb.2017.09.032
Received 21 July 2017; Received in revised form 11 September 2017; Accepted 12 September 2017
Available online 14 September 2017

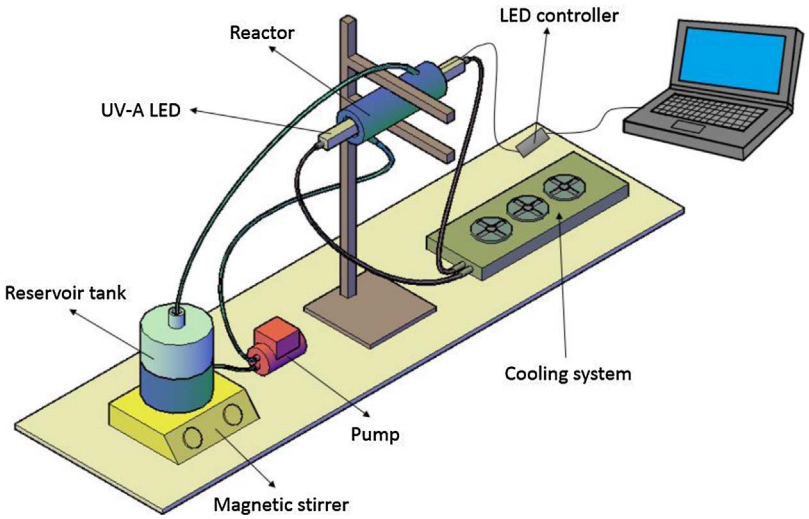

Fig. 1. Schematic representation of the experimental setup.

peaks at different wavelengths were used to determine the action spectra. Taking into account that several authors have pointed out the existence of certain differences between the photocatalytic oxidation of organics and the inactivation of microorganisms [22,23] two different model reactions were selected in order to evaluate the efficiency of each system. The photocatalytic oxidation of methanol to formaldehyde was used as model chemical reaction, whereas *E. coli* was selected as model pathogenic microorganism for disinfection applications. Finally, based on the action spectra, prediction of the process efficiency under solar light irradiation were carried out, being successfully validated by experimental data.

2. Material and methods

2.1. Experimental setup

An annular photoreactor 15 cm length, 3 cm internal diameter and 5 cm external diameter (Fig. 1) was used to get the experimental data to calculate the photonic efficiency data. The reactor was operated in a closed recirculating circuit driven by a centrifugal pump with a reservoir tank, being the total working volume of 1 L. As illumination sources, six different 8-UV-A LED based systems providing maximum emission peaks centered at different wavelengths (Fig. 2) were placed in the axis of the annular photoreactor. The LED-based systems were continuously refrigerated using a liquid cooling system (Koolance EX2-755) and the irradiation power was controlled through the electrical current intensity using the software Eldoled LED driver configuration Toolbox. Potassium ferrioxalate actinometry experiments were carried out in each case in order to calculate the total irradiation power as described elsewhere [24].

2.2. Experimental procedure

Chemical oxidation experiments were carried out using methanol (Sigma-Aldrich, LC–MS) as model of chemical pollutant. The initial concentration was fixed at 100 mM and all solutions were prepared in deionized water. Methanol oxidation was followed through the colorimetric determination of the formaldehyde produced throughout the reaction [25,26], quantitative oxidation product when methanol is in excess [27,28].

As model of microorganism, *Escherichia coli* K12 strains (CECT 4624, corresponding to ATCC 23631, where CECT stands for "Colección Española de Cultivos Tipo") were used. Fresh liquid cultures were prepared by inoculation in a Luria-Bertani (LB) nutrient medium (Miller's LB Broth, Scharlab) and incubation at 37 °C for 24 h under constant stirring on a rotary shaker. In all the experiments, the bacterial suspensions (NaCl 0.9%) were prepared with an initial concentration of 10^6 CFU/mL.

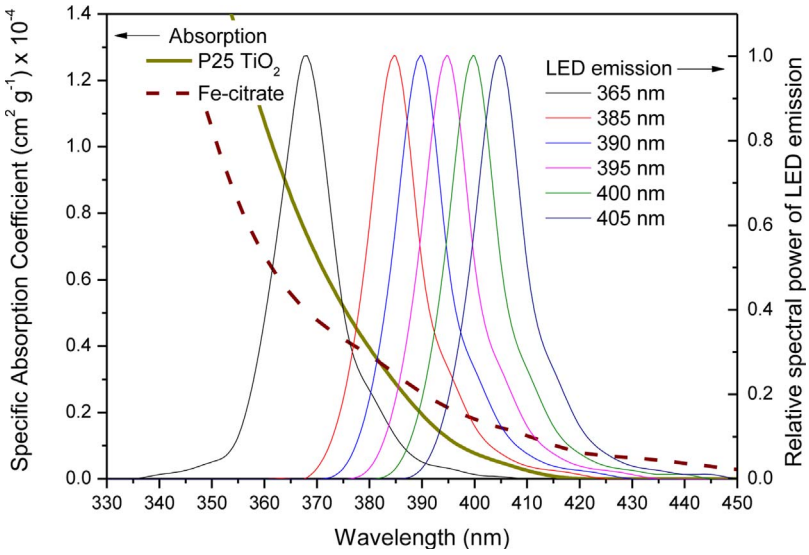

Fig. 2. Spectral emission of the light sources and specific absorption coefficients for TiO_2 and Fe-citrate complex.

The analysis of the samples was carried out throughout the reaction following a standard serial dilution procedure. Each decimal dilution was spotted 4 times on LB nutrient agar plates and incubated at 37 °C for 24 h before counting. To check the reproducibility, all the experiments were replicated at least twice. The results were calculated as the mean of the replicates and the experimental errors as the standard deviation.

2.3. Catalyst

Two different catalysts with different absorption spectra were used at neutral pH. Commercial Evonik P25 titanium dioxide (surface area of ca. 50 m^2 /g) was used in a heterogeneous photocatalytic process at a concentration value of 100 mg /L, previously optimized [29]; Fe-citrate complex CAS number 3522-50-7 (Sigma-Aldrich) was used to carry out a photo-Fenton process at a concentration value of 10 mg /L relative to the Fe-citrate content as it has been previously reported by other authors [16]. In all the photo-Fenton experiments, a concentration of hydrogen peroxide 10 times higher than the concentration of Fe-citrate was preliminary optimized to ensure no depletion throughout the reaction. The specific absorption coefficients of Fe-citrate were calculated using the absorbance measured in a UV/vis spectrophotometer (Biochrom Libra S22) and are shown in Fig. 2. On the other hand the specific absorption coefficients of P25 TiO_2 were taken from literature [30] and are also shown in Fig. 2.

2.4. Solar irradiation

In order to validate the predictions of the expected photocatalytic activity under solar light, both methanol oxidation and bacterial inactivation experiments were carried out with solar light using a Compound Parabolic Collector (CPC) reactor. The CPC reactor has two differentiated circuits in which experiments were carried out simultaneously with Fe-citrate and P25 TiO_2. Each circuit has a borosilicate 3.3 Duran® glass tube (inner diameter of 26 mm) with a length of 380 mm placed in the focal line of the CPC collector [31]. The reactor was operated in a closed recirculating circuit driven with a reservoir tank, being the total working volume of 1 L. The experiments were carried in July 2017 at Universidad Rey Juan Carlos facilities in Mostoles, Spain (40.33°N, 3.88°W). The solar irradiance was monitored during the reaction time with a spectrophotometer (Blue Wave, StellarNet Inc.).

3. Results

3.1. Incident radiation and power consumption

Actinometrical experiments were carried out to determine the total amount of photons incident to the reactor volume for different electrical power consumptions. As it is well known, an increase in the electrical current of LED causes an increase in the emitted light. However, the efficiency in terms of photons produced per unit of electrical energy consumed is not the same for LEDs emitting at different wavelengths. In Fig. 3 it can be seen how the LEDs centered at higher wavelengths have the greatest energy efficiencies in terms of moles of photons (Einstein, E) per unit of electrical power. Values of 3.75, 4.87, 4.95, 5.54, 5.92 and 6.78 E/kWh were obtained for LED with emission peaks centered at 365, 385, 390, 395, 400 and 405 nm, respectively.

Taking into account the previous results and the fact that most of the photocatalytic processes use artificial light sources centered at 365 nm it is particularly interesting to search for alternative processes that use catalysts working at larger values of wavelength resulting in significant energy savings.

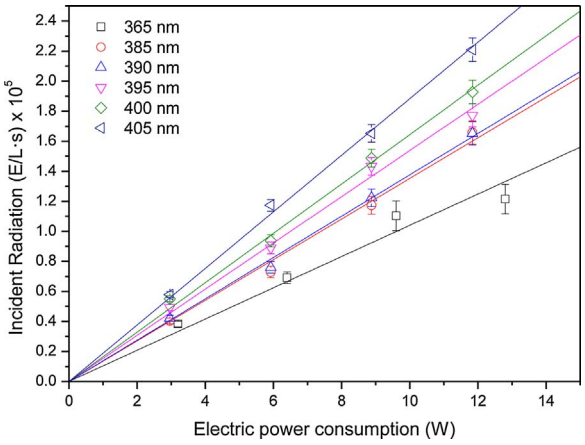

Fig. 3. Incident radiation versus power consumption for different LED sources.

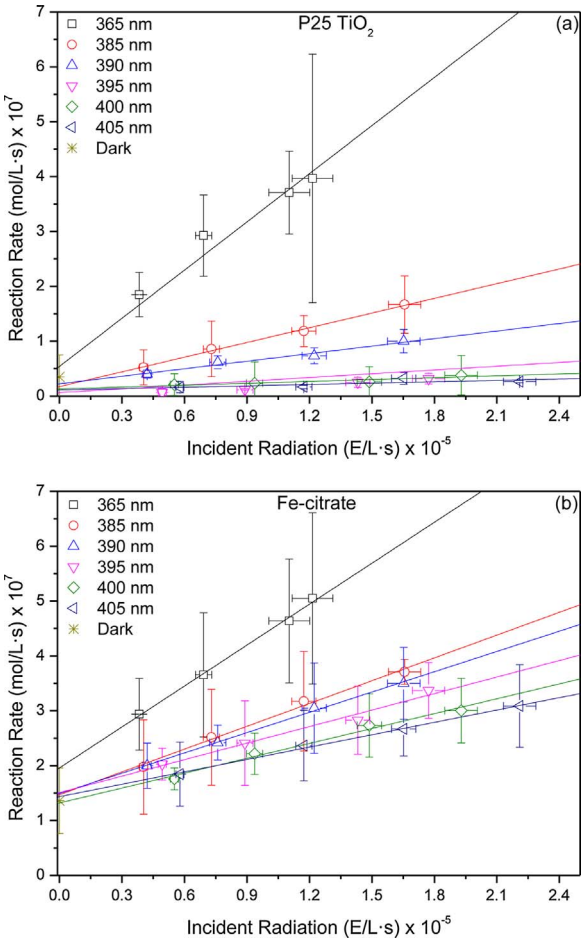

Fig. 4. Reaction rate of formaldehyde formation versus incident radiation for different wavelengths.

3.2. Action spectra for methanol oxidation

Oxidation of methanol to formaldehyde was selected as model reaction to study the efficiency of the processes. The mechanism of the oxidation via ·OH radical have been established in the literature [25,26], being demonstrated that under the operational conditions used in this work the formation of formaldehyde as product can be considered quantitative [28,26]. Reaction rate values can be calculated from the profiles of the formaldehyde formation versus time, as detailed in previous studies [27,32]. The reaction rate values of formaldehyde

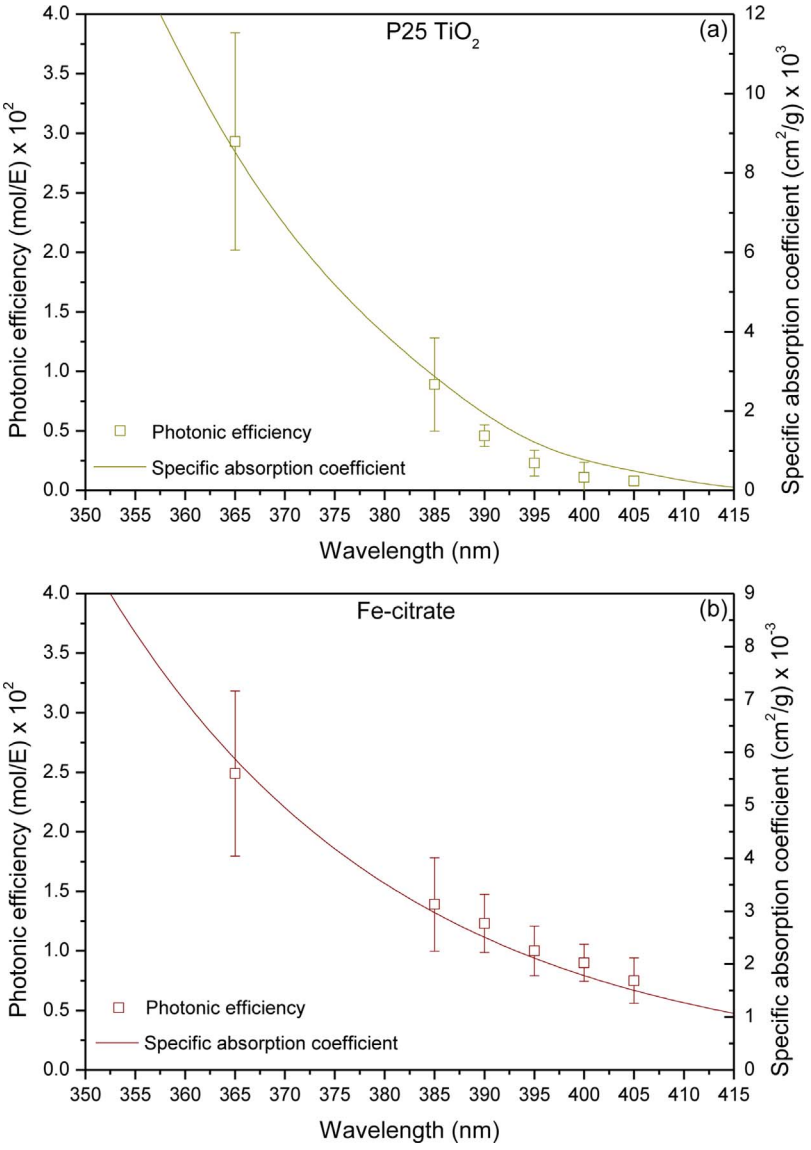

Fig. 5. Action spectra of the photocatalysts in terms of photonic efficiency of methanol oxidation, and spectral specific absorption coefficients for (a) P25 TiO_2 and (b) Fe-citrate.

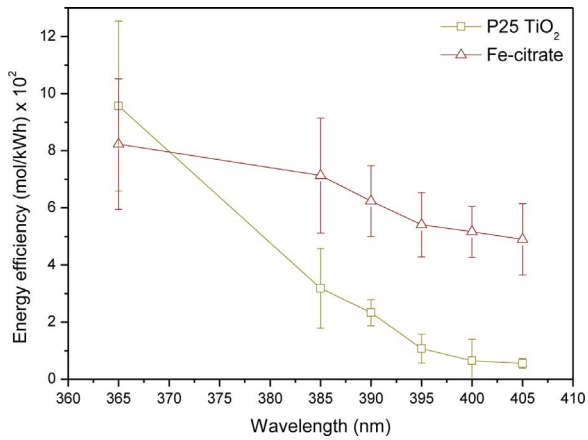

Fig. 6. Energy efficiency of methanol oxidation versus wavelength for P25 TiO_2 and Fe-citrate.

formation using different light sources with emission centered at different wavelength are shown in Fig. 4. As already observed in a previous work [13], there is a linear dependence between the reaction rate and the incident radiation that allow tuning the process with the regulation of the electrical intensity powering the LEDs. The differences observed between the photocatalytic process with P25 TiO_2 and the photo-Fenton process with Fe-citrate are more noticeable. In the case of P25 TiO_2, it can be seen how the highest values of reaction rate are obtained when the LED centered at 365 nm are used. However, as the wavelength increases, a very pronounced drop occurs with negligible formaldehyde formation occurring at wavelengths above 390 nm. The behavior with Fe-citrate is very different. Although as with P25 TiO_2 the maximum reaction rate is reached with the LED centered at 365 nm, the increase in wavelength does not produce such a pronounced drop in the reaction rate, being possible to observe a considerable methanol oxidation when using LEDs centered a 405 nm.

The behavior observed in Fig. 4 can be easily explained by taking into account the absorption spectra of the two catalysts used. In Fig. 5 are plotted the specific absorption coefficients [30] and the photonic efficiency as a function of wavelength where photonic efficiency was calculated as the ratio between the mol of formaldehyde formed and the Einsteins reaching the reactor. It can be seen how in both cases the photonic efficiency obtained for each wavelength perfectly matches the absorption spectrum of the catalyst. This is a very important aspect to take into account since it allows estimation of the photonic efficiency for different wavelengths based on the absorption spectrum without being required performing new experiments. Although this fact has

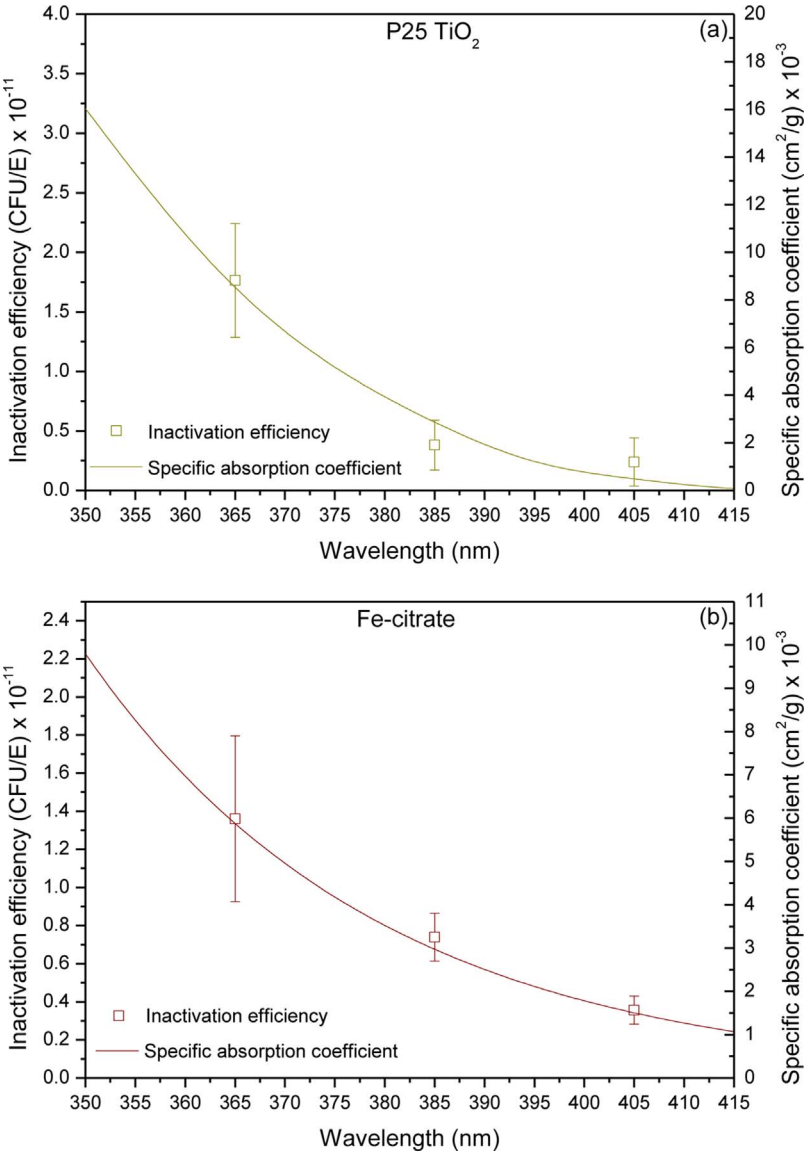

Fig. 7. Inactivation efficiency and spectral specific absorption coefficients for (a) P25 TiO_2 and (b) Fe-citrate.

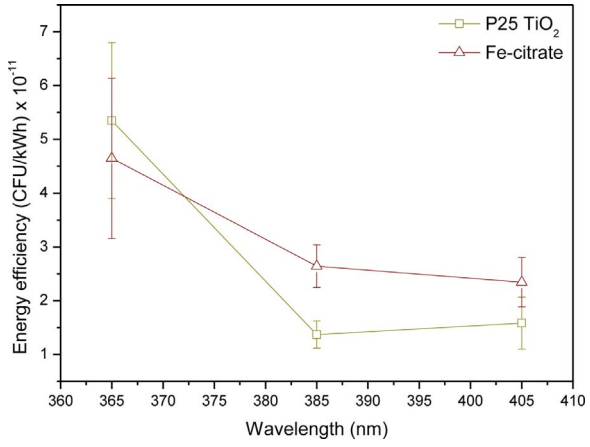

Fig. 8. Energy efficiency of bacterial inactivation versus wavelength for P25 TiO_2 and Fe-citrate.

been widely assumed in the literature, this work provides the quantitative data to support this assumption.

However, the most important aspect to take into account when using artificial lighting sources is the energy consumption of the system. Fig. 6 shows the energy efficiency of the two catalysts for the selected concentrations, calculated as the mol of formaldehyde formed per kWh of electrical energy consumed, as a function of wavelength. It can be observed how in the case of P25 TiO_2 due to the great drop in photonic efficiency when increasing wavelength, the LEDs of 365 nm are still clearly the most recommended to use despite the fact that they are energetically less efficient. In the case of Fe-citrate, there is no such a clear difference between LED centered at different wavelengths. The worst photonic efficiency for LED emitting at longer wavelengths is partially compensated by its better efficiency in the conversion of electricity to photons [15].

This study has been limited to the UV-A wavelength range with practical applications with the current state of the art of LED devices. The use of wavelengths below 365 nm is limited by the low efficiency and very high cost of this type of LED devices. On the other hand, the high energy efficiency of visible light LED no longer compensates the low absorption of TiO_2 on this spectral range. Anyway, the reported procedure could be easily extrapolated to other LED and catalysts available in the future.

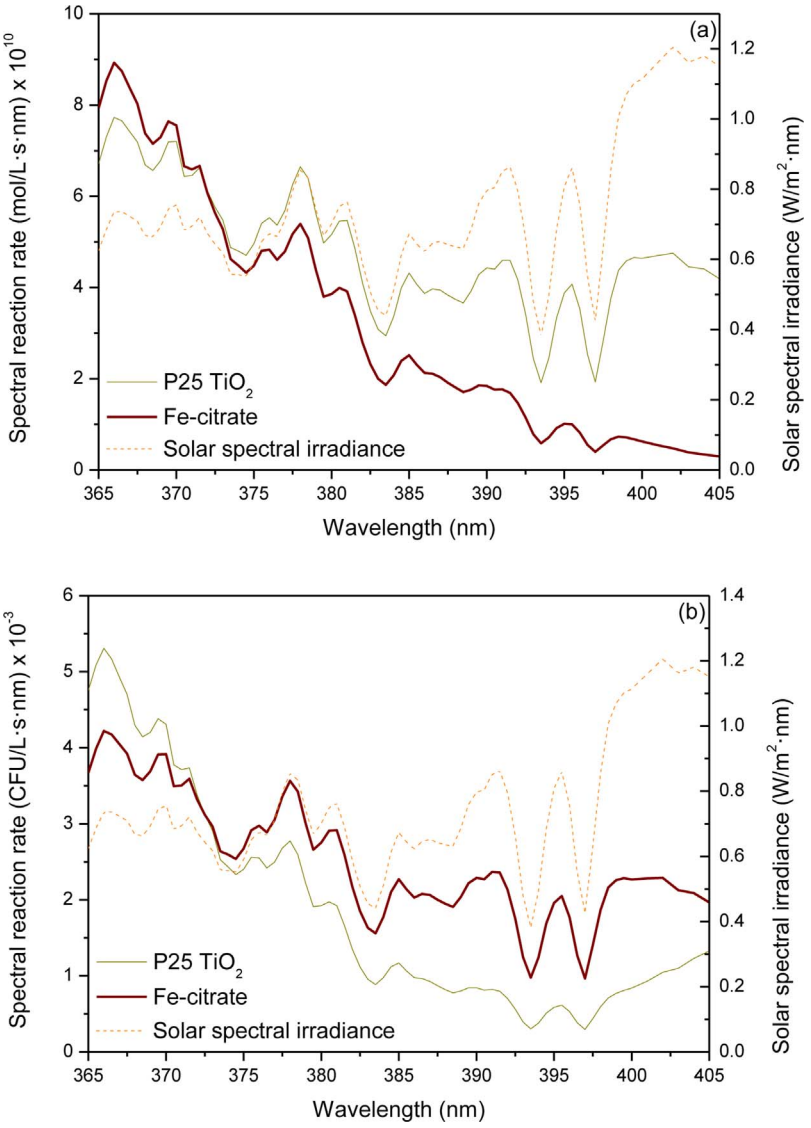

Fig. 9. Estimation of the spectral reaction rate for (a) methanol oxidation and (b) bacterial inactivation for standard AM 1.5 solar illumination for P25 TiO_2 and Fe-citrate.

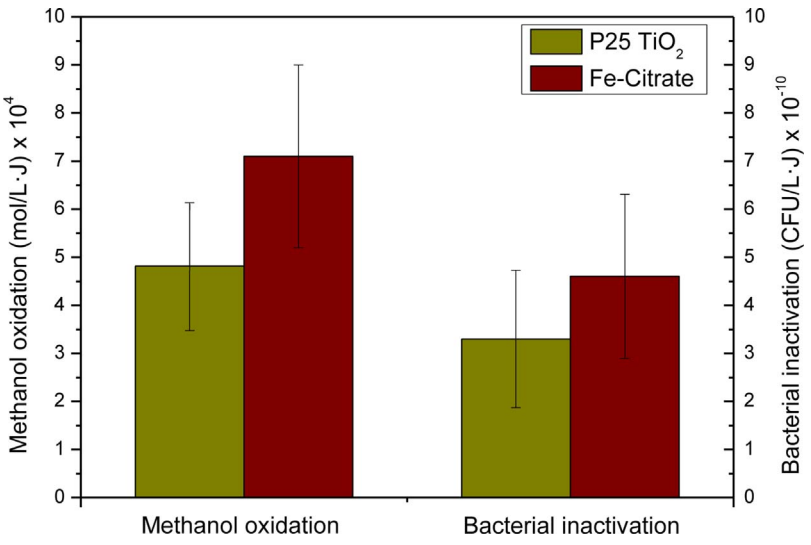

Fig. 10. Reaction rate of methanol oxidation and bacterial inactivation under sunlight.

3.3. Bacterial inactivation

Similar experiments to those previously carried out for methanol oxidation were carried out to study bacterial inactivation. The inactivation profiles were fitted using a mechanistic model based on a series-event mechanism for the cumulative attached of reactive oxygen species to the viable bacteria until their complete inactivation [23]. The inactivation efficiencies of each catalyst for the selected concentrations depicted in Fig. 7 were calculated as the ratio of the inactivated CFU per Einstein reaching the reactor. As for methanol oxidation, the inactivation efficiency is in perfect agreement with the absorption spectra of the catalysts. These results show that the only step for both bacterial inactivation and chemical oxidation dependent of the wavelength is the generation of electron-hole pairs whereas the remaining steps only depend on the oxidative capacity of the hydroxyl radicals generated.

Regarding the energy efficiency, in Fig. 8 it can be observed how the results agree again with those obtained for the methanol oxidation. For the chosen catalysts concentrations, the highest energy efficiency is obtained for the LED of 365 nm when P25 TiO_2 is used. On the other hand, when using LEDs with longer wavelengths it is more cost effective to use Fe-citrate as a catalyst.

3.4. Solar irradiation

A particularly interesting option for the application of photocatalytic processes is the use of solar irradiation. Due to the polychromatic nature of the solar light, a predictive estimation of the activity required the discretization of the solar spectrum and the estimation of the photonic efficiency of the process for each individual wavelength. Afterwards, the integration over the whole wavelength range would lead to the estimation of the global efficiency. The photonic efficiency for each individual wavelength in the 365–405 nm range have been calculated by interpolation of the results shown in Fig. 5 for methanol oxidation and in Fig. 7 for bacterial inactivation. Fig. 9 shows the solar AM 1.5 reference spectrum based on the ASTM G173-03 standard [33] and the reaction rate for methanol oxidation and bacterial inactivation calculated for each wavelength considering the action spectra of the two catalysts. By performing the integral of each function, it is possible to obtain the global reaction rate estimated for the studied range of wavelengths. Values of 1.27×10^{-8} and 1.92×10^{-8} mol/L s were obtained for methanol oxidation with P25 TiO_2 and Fe-citrate, respectively, whereas values of 7.38×10^{4} and 1×10^{5} CFU/L s were obtained for bacterial inactivation. That means that when 10 mg/L of Fe-citrate is used under UV-A solar irradiation, it is expected a 50% higher activity for methanol oxidation and 35% higher activity for bacterial inactivation than when 100 mg/L of P25 TiO_2 is used, being these quantitative improvement values linked to the specific concentrations used in these experiments. In any case, it can be concluded that there is an improvement in both bacterial inactivation and chemical oxidation with the use of Fe-citrate with sunlight compared to the traditional use of P25 TiO_2, which makes it a very attractive alternative to improve the efficiency of photocatalytic processes with sunlight.

In order to validate these predictions, experiments of methanol oxidation and bacterial inactivation were carried out in a CPC reactor under sunlight on different days of June 2017 at Universidad Rey Juan Carlos facilities in Móstoles, Spain (40.33°N, 3.88°W). The reaction rates in each case were calculated taking into account the solar radiation accumulated throughout the experiments and their average value is represented in Fig. 10. These results show improvements of 38 and 39% for methanol oxidation and bacterial inactivation, respectively when 100 mg/L of TiO_2 and 10 mg/L of Fe-Citrate are used, which confirm the predicted improvement with the use of Fe-citrate. The differences between the values of the relative enhancement of the experimental data and predicted based on the action spectra are reasonable considering that predictions have been based exclusively with experimental efficiencies in the 365–405 nm wavelength range. The availability of the action spectra in the full spectral range of the solar light should obviously lead to a more rigorous estimation. Anyway, the low absorbance of both catalysts above 405 nm, and the low solar irradiance below 365 nm reasonable justify this assumption, which has been indeed validated by the experimental data.

4. Conclusions

The use of monochromatic LED sources has been proved a useful tool for the determination of the action spectra of photocatalytic processes. Experimental data confirm the direct relation between the photonic efficiency and the absorption spectra of TiO_2 and Fe-citrate photocatalysts for both chemical oxidation and bacterial inactivation model reactions.

The maximum energy efficiency when using P25 TiO_2 has been reached with the LED system emitting at 365 nm, showing a drastic drop in efficiency resulting in completely inefficient systems when the wavelength increases. A very different behavior is obtained with the iron citrate complex, not showing such a pronounced drop in photonic efficiency when the wavelength is increased. This fact, together with the fact that LEDs with values of wavelength close to the visible range have a significantly higher energy efficiency raise the possibility of using near-visible wavelengths for chemical oxidation and bacterial inactivation in an economically viable way.

Predictions of the process efficiency under solar irradiation based on the action spectra determined with LED at lab scale have been successfully validated by experimental data. Although the absolute values of the activity depend on the catalyst loading, reactor design and irradiance level, the methodology proposed in this work could be easily extrapolated to other wavelength ranges required by novel catalysts or efficient short wavelength monochromatic LED sources that could be available in the future.

Acknowledgements

The authors gratefully acknowledge the financial support of the Spanish Ministry of Economy and Competitiveness (MINECO), in the frame of the collaborative international consortium WATERJPI2013–MOTREM of the Water Challenges for a Changing World Joint Programming Initiative (Water JPI) Pilot Call. This work has been also partially funded by Comunidad de Madrid through the program REMTAVARES (S2013/MAE-2716). Miguel Martín Sómer also acknowledges MICINN for the FPU grant (FPU014/04389).

References

[1] C. Su, C.M. Tseng, L.F. Chen, B.H. You, B.C. Hsu, S.S. Chen, Sol-hydrothermal preparation and photocatalysis of titanium dioxide, Thin Solid Films 498 (2006) 259–265.
[2] M.R. Hoffmann, S.T. Martin, W. Choi, D.W. Bahnemann, W.M. Keck, Environmental applications of semiconductor photocatalysis, Chem. Rev. 95 (1995) 69–96.
[3] R. Quesada-Cabrera, A. Mills, C. O'Rourke, Action spectra of P25 TiO_2 and a visible light absorbing, carbon-modified titania in the photocatalytic degradation of stearic acid, Appl. Catal. B Environ. 150 (2014) 338–344.
[4] D.Y. Goswami, A review of engineering developments of aqueous phase solar photocatalytic detoxification and disinfection processes, J. Sol. Energy Eng. 119 (1997) 101–107.
[5] D. Spasiano, R. Marotta, S. Malato, P. Fernández-Ibañez, I. Di Somma, Solar photocatalysis: materials, reactors, some commercial, and pre-industrialized applications. A comprehensive approach, Appl. Catal. B Environ. 170–171 (170) (2015) 90–123.
[6] X.H. Wang, J.G. Li, H. Kamiyama, Y. Moriyoshi, T. Ishigaki, Wavelength-sensitive photocatalytic degradation of methyl orange in aqueous suspension over iron(III)-doped TiO_2 nanopowders under UV and visible light irradiation, J. Phys. Chem. B 110 (2006) 6804–6809.
[7] H. Irie, Y. Watanabe, K. Hashimoto, Carbon-doped anatase TiO_2 powders as a visible-light sensitive photocatalyst, Chem. Lett. 32 (2003) 772–773.
[8] T. Ohno, T. Mitsui, M. Matsumura, Photocatalytic activity of S-doped TiO_2 photocatalyst under visible Light, Chem. Lett. 32 (2003) 364–365.
[9] Y. Sakatani, J. Nunoshige, H. Ando, K. Okusako, H. Koike, T. Takata, J.N. Kondo, M. Hara, K. Domen, Photocatalytic decomposition of acetaldehyde under visible

light irradiation over La^{3+} and N co-doped TiO_2, Chem. Lett. 32 (2003) 1156–1157.
[10] K. Song, M. Mohseni, F. Taghipour, Application of ultraviolet light-emitting diodes (UV-LEDs) for water disinfection: a review, Water Res. 94 (2016) 341–349.
[11] M.A.S. Ibrahim, J. MacAdam, O. Autin, B. Jefferson, Evaluating the impact of LED bulb development on the economic viability of ultraviolet technology for disinfection, Environ. Technol. 35 (2014) 400–406.
[12] M.A. Wü Rtele, T. Kolbe, M. Lipsz, A. Kü Lberg, M. Weyers, M. Kneissl, M. Jekel, Application of GaN-based ultraviolet-C light emitting diodes e UV LEDs e for water disinfection, Water Res. 45 (2011) 1481–1489.
[13] M. Martín-Sómer, C. Pablos, R. van Grieken, J. Marugán, Influence of light distribution on the performance of photocatalytic reactors: LED vs mercury lamps, Appl. Catal. B Environ. 215 (2017) 1–7.
[14] J. Rodríguez-Chueca, C. Amor, J.R. Fernandes, P.B. Tavares, M.S. Lucas, J.A. Peres, Treatment of crystallized-fruit wastewater by UV-A LED photo-Fenton and coagulation–flocculation, Chemosphere 145 (2016) 351–359.
[15] I. de la Obra, B. Esteban García, J.L. García Sánchez, J.L. Casas López, J.A. Sánchez Pérez, Low cost UVA-LED as a radiation source for the photo-Fenton process: a new approach for micropollutant removal from urban wastewater, Photochem. Photobiol. Sci. 16 (2017) 72–78.
[16] C. Ruales-Lonfat, J.F. Barona, A. Sienkiewicz, J. Vélez, L.N. Benítez, C. Pulgarín, Bacterial inactivation with iron citrate complex: a new source of dissolved iron in solar photo-Fenton process at near-neutral and alkaline pH, Appl. Catal. B Environ. 180 (2016) 379–390.
[17] L. Clarizia, D. Russo, I. Di Somma, R. Marotta, R. Andreozzi, Homogeneous photo-Fenton processes at near neutral pH: a review, Appl. Catal. B Environ. 209 (2017) 358–371.
[18] J. Rodríguez-Chueca, C. Amor, T. Silva, G. Li Puma, M.S. Lucas, J.A. Peres, Treatment of winery wastewater by sulphate radicals: HSO^{5-}/transition metal/UV-A LEDs, Chem. Eng. J. 310 (2017) 473–483.
[19] M.R.A. Silva, A.G. Trovó, R.F.P. Nogueira, Degradation of the herbicide tebuthiuron using solar photo-Fenton process and ferric citrate complex at circumneutral pH, J. Photochem. Photobiol. A Chem. 191 (2007) 187–192.
[20] H. Katsumata, S. Kaneco, T. Suzuki, K. Ohta, Y. Yobiko, Photo-Fenton degradation of alachlor in the presence of citrate solution, J. Photochem. Photobiol. A Chem. 180 (2006) 38–45.
[21] S. Miralles-Cuevas, I. Oller, J.A. Sánchez Pérez, S. Malato, Removal of pharmaceuticals from MWTP effluent by nanofiltration and solar photo-Fenton using two different iron complexes at neutral pH, Water Res. 64 (2014) 23–31.
[22] J. Marugán, R. van Grieken, C. Pablos, C. Sordo, Analogies and differences between photocatalytic oxidation of chemicals and photocatalytic inactivation of microorganisms, Water Res. 44 (2010) 789–796.
[23] J. Marugán, R. van Grieken, C. Sordo, C. Cruz, Kinetics of the photocatalytic disinfection of *Escherichia coli* suspensions, Appl. Catal. B Environ. 82 (2008) 27–36.
[24] C.G. Hatchard, C.A. Parker, A new sensitive chemical actinometer. II. potassium ferrioxalate as a standard chemical actinometer, Proc. R. Soc. Lond. Ser. A. Math. Phys. Sci. 235 (1956) 518 (LP-536).
[25] J. Marugán, D. Hufschmidt, M.J. López-Muñoz, V. Selzer, D. Bahnemann, Photonic efficiency for methanol photooxidation and hydroxyl radical generation on silica-supported TiO_2 photocatalysts, Appl. Catal. B Environ. 62 (2006) 201–207.
[26] C. Casado, J. Marugán, R. Timmers, M. Muñoz, R. van Grieken, Comprehensive multiphysics modeling of photocatalytic processes by computational fluid dynamics based on intrinsic kinetic parameters determined in a differential photoreactor, Chem. Eng. J. 310 (2017) 368–380.
[27] C. Pablos, J. Marugán, R. van Grieken, C. Adán, A. Riquelme, J. Palma, Correlation between photoelectrochemical behaviour and photoelectrocatalytic activity and scaling-up of P25-TiO_2 electrodes, Electrochim. Acta 130 (2014) 261–270.
[28] L. Sun, J.R. Bolton, Determination of the quantum yield for the photochemical generation of hydroxyl radicals in TiO_2 suspensions, J. Phys. Chem. 100 (1996) 4127–4134.
[29] R. van Grieken, J. Marugán, C. Sordo, C. Pablos, Comparison of the photocatalytic disinfection of *E. coli* suspensions in slurry, wall and fixed-bed reactors, Catal. Today 144 (2009) 48–54.
[30] M.L. Satuf, R.J. Brandi, A.E. Cassano, O.M. Alfano, Experimental method to evaluate the optical properties of aqueous titanium dioxide suspensions, Ind. Eng. Chem. Res. 44 (2005) 6643–6649.
[31] K.K. Philippe, R. Timmers, R. Van Grieken, J. Marugán, Photocatalytic disinfection and removal of emerging pollutants from effluents of biological wastewater treatments, using a newly developed large-scale solar simulator, Ind. Eng. Chem. Res. 55 (2016) 2952–2958.
[32] J. Marugán, R. Van Grieken, C. Pablos, C. Adán, R. Timmers, Determination of photochemical, electrochemical and photoelectrochemical efficiencies in a photoelectrocatalytic reactor, Int. J. Chem. React Eng. 11 (2013) 787–797.
[33] ASTM G173-03 Standard solar spectral irradiance AM 1.5, http://rredc.nrel.gov/solar/spectra/am1.5/ (accessed Sept 13, 2017).